Contents lists available at ScienceDirect

Heliyon

journal homepage: www.cell.com/heliyon

Research article

Dynamics of atmospheric emissions and meteorological variables in Bangladesh from pre-to post-COVID-19 lockdown

Md. Tushar Ali [*], Islam M. Rafizul, Quazi Hamidul Bari

Department of Civil Engineering, Khulna University of Engineering & Technology (KUET), Khulna-9203, Bangladesh

ABSTRACT

Following the COVID-19 restrictions, there was a sharp decline in global air quality and related environmental metrics. Due to the limited availability of in situ atmospheric data in Bangladesh, this study collected data on various air pollutants (NO_2, SO_2, CO, and $PM_{2.5}$), greenhouse gases (CO_2, CH_4, and O_3), as well as meteorological variables like Land Surface Temperature (LST), Relative Humidity (RH), Precipitation, surface albedo and Aerosol Optical Depth (AOD) from different datasets by Google Earth Engine (GEE), the International Energy Agency (IEA), NASA Giovanni, and NASA Power Access Viewer, covering periods before (2019), during (2020), and after (2021–2023) the COVID-19 lockdown in Bangladesh. GIS-based assessment alongside Principal Component Analysis (PCA) has been performed to explore the patterns, trends and correlations among the observed variables. Results showed in 2020 compared to 2019, NO_2, SO_2, CO, $PM_{2.5}$, and CO_2 concentrations decreases by 1.94, 16.67, 1.95, 2.08, and 6 %, respectively, while CH_4 and O_3 continued to rise. Meteorological variables exhibited a 0.16 °C decreases in LST, 6.4 % increases in RH, a 6 % reduction in AOD, and 6.36 % declines in surface albedo. Post-lockdown in 2021, air pollutants surged (NO_2, SO_2, CO, and $PM_{2.5}$ increases by 17.3, 23.6, 0.6, and 8.3 %, respectively), with CO_2, LST, and AOD rising by 8.5 %, 0.13 °C, and 8.3 %, and a slight 0.46 % decrease in RH compared to 2019 due to resuming more economic activities, transportation and industrial production works. The years 2022–2023 saw slight improvements in most variables except CH_4, though concentrations did not revert to those of 2019. The findings of correlation coefficients revealed that pollutants and GHG are highly correlated with the meteorological variables specially with RH. This study underscores the substantial shifts in atmospheric variables from pre-to post-lockdown periods, offering valuable insights for more effective management of the greenhouse effect and air pollution control strategies.

1. Introduction

On December 31, 2019, the first human cases of a severe acute respiratory syndrome coronavirus (SARS-CoV-2), known as COVID-19, were detected in Wuhan City, China [1–3]. The World Health Organization (WHO) declared the novel coronavirus disease a pandemic on March 11, 2020 [4]. Globally, there have been 704,753,890 confirmed coronavirus cases, 7,010,681 deaths, and 75,619, 811 recoveries [5]. As of May 19, 2024, Bangladesh has a population of 174,492,465, ranking 8th globally, with a density of 1329 people per km^2, 40.9 % urban population, a median age of 27.1 years, and a total land area of 130,170 km^2 and there have been 2,049,

377 coronavirus cases and 29,493 deaths [5,6].

Urban air quality has emerged as a critical concern for city dwellers worldwide, driven by its profound impacts on health, ecology, and climate change [7–9]. As urban development intensifies, the associated risks increase [10], further complicating efforts to mitigate air quality issues. Additionally, bioclimate comfort varies across different altitudes and land uses within urban areas, influencing the overall livability of cities [11]. Notably, bio-comfort is closely tied to air quality conditions, underscoring the interconnectedness of environmental factors and human well-being in urban settings [12]. Unfortunately, the COVID-19 lockdowns, which significantly limited human activities, can be viewed as a naturally controlled experiment with notably reduced air pollutant emissions. However, the formation of atmospheric pollutants remains complex, influenced by emissions and meteorological conditions [13–15]. This restriction worldwide has notably enhanced air quality, wildlife sightings, water quality, and reduced noise pollution; however, challenges such as increased non-biodegradable waste from surgical masks and protective equipment usage persist during the pandemic [16–18].

During the lockdowns in Wuhan, China (starting January 23, 2020) and Southampton, UK (starting March 23, 2020), nitrogen dioxide (NO_2) concentrations dropped by nearly 63 % and 92 %, respectively, and particulate matter (PM) in Wuhan reduced by 35 %, with minimal effects on sulfur dioxide (SO_2) and carbon monoxide (CO) compared to the same period from 2017 to 19 [19]. In that time, NO_2 concentrations decreased while O_3 concentrations consistently increased at all stations, a paradoxical situation since O_3 is formed through photochemical reactions involving NOx and volatile organic compounds [20]. In the UK, overall traffic was reduced by 69 %, resulting in mean NO_2 reductions of 38.3 % and $PM_{2.5}$ reductions of 16.5 %, while O_3 concentrations increased by 7.6 % compared to the same period during 2017–19 [21]. Another study [22] in Six Megacities in China shows that the lockdown reduced ambient NO_2 concentrations by 36–53 % during the most restrictive periods but also led to increased O_3 concentrations. By analyzing the air quality data from 87 of the world's capital, industrial, and polluted cities, in 2020, AQI-$PM_{2.5}$, AQI-PM10, and AQI-NO_2 decreased by 7.36 %, 17.52 %, and 20.54 % respectively, compared to 2019, but in 2021, they increased by 4.25 %, 9.08 %, and 7.48 %, with temperature and relative humidity inversely correlating with these AQI measures [23].

Urban heat islands (UHIs), a significant human-driven climate alteration, have become a critical issue globally, drawing substantial research attention in recent times [24–27]. Previous research has highlighted notable reductions in UHIs and Land Surface Temperature (LST) in various cities, including Tehran [28], New Delhi [29], and major cities in the Middle East [30]. Between 2013 and 2022, a study in Turkey examined LST and UHI alongside their influencing parameters through remote sensing techniques [31]. During lockdown periods in China, over 300 megacities experienced a reduction in surface UHI intensity by 0.25 K during the day and 0.23 K at night, compared to reference periods [32]. Similarly, a linear regression analysis conducted over the last 30 years in Turkey identified the factors associated with LST, normalized difference vegetation index (NDVI), and normalized difference built-up index (NDBI) [33]. Another study noted the impact of vegetation and built-up areas on LST, as well as the effects of LST on human health, emphasizing the intricate relationship between urban development and environmental health [34]. Furthermore, research in megacities across Pakistan shows that limitations on transportation within urban areas led to a noticeable reduction in LST [35].

Bangladesh's economic growth, among the fastest globally, is heavily driven by industrial expansion, with the industrial sector contributing over 35 % to GDP and averaging a 13 % annual growth rate [36,37]. The Government of Bangladesh (GoB) declared special "general leave" from 26 March in the name of "lockdown" and extended it up to May 30, 2020 in seven different time slots [38]. The period from December 2020 to the end of February 2021 saw the lowest rate of infections since the outbreak of the pandemic. The positivity rates remained below five percent for the first time from mid-January to early March [39]. The lockdown restrictions in Bangladesh from February 1 to May 30 of 2019 and 2020, SO_2 and NO_2 concentrations dropped by 43 % and 40 % respectively, while tropospheric O_3 increased by over 7 % [40]. The major cities of Bangladesh have seen a notable rise in the number of motorized vehicles increasing each year. In Dhaka, for example, the motor vehicle population has surged significantly, with growth rates of 7–16 % over the past decade [41]. Consequently, these urban centers have encountered significant air pollution challenges compared to other regions of the country [42]. Dhaka, in particular, stands out as one of the most polluted cities nationally and ranks as the third most polluted megacity globally [43,44]. In this city, ground- and satellite-based data from March 8 to May 15, 2020, showed declines of 26 % ($PM_{2.5}$), 20.4 % (NO_2), 17.5 % (SO_2), 9.7 % (O_3), and 8.8 % (CO) during the partial and full lockdown compared to the pre-lockdown period [45].

Existing research worldwide, including in Bangladesh, has yet to comprehensively address the combined effects of post-lockdown years of COVID-19 on air pollutants, greenhouse gases, and meteorological variables. This study aims to conduct a thorough remote sensing-based analysis of changes in air pollutants (NO_2, SO_2, CO, and $PM_{2.5}$), greenhouse gases (CO_2, CH_4, and O_3) meteorological variables (LST, RH, Precipitation, surface albedo, and AOD) in Bangladesh by comparing data from before, during, and after the years of COVID-19 lockdown to understand the impact of lockdowns on environmental dynamics and average in their concentrations. Additionally, this study uses Principal Component Analysis (PCA) to examine the interrelationships among atmospheric variables, identifying the strength and direction (positive or negative) of correlations. The approach provides a clearer understanding of how these variables interact, highlighting key drivers of atmospheric variability.

2. Methodology adopted

2.1. Study area

Bangladesh, officially known as the People's Republic of Bangladesh, is located in South Asia at 24° 00′ N latitude and 90° 00′ E longitude shown in Fig. 1. It ranks as the eighth-most populous country globally and is one of the most densely populated, with nearly 170 million people living in an area of 148,460 square kilometers (57,320 square miles). This results in a population density of 1156.84

people per square kilometer. Dhaka, the capital and largest city, is the country's political, industrial, financial, and cultural hub. Bangladesh has a tropical climate, featuring a mild winter from October to March and a hot, humid summer from March to June. The country has never experienced temperatures below 0 °C (32 °F), with the lowest recorded temperature being 1.1 °C (34.0 °F) in Dinajpur on February 3, 1905 [46].

A hot and humid monsoon season prevails from June to October, bringing most of the country's rainfall. Bangladesh is notably one of the most climate change-vulnerable nations, facing natural disasters like floods, tropical cyclones, tornadoes, and tidal bores nearly yearly [47–49]. Vehicular air pollution significantly contributes to respiratory issues in urban Bangladesh. A World Bank report indicates that air pollution causes 15,000 deaths annually in the country. The National Institute of Diseases of the Chest and Hospital (NIDCH) (https://www.nidch.gov.bd/overviews) states that nearly seven million people in Bangladesh suffer from asthma, with over half of them being children.

2.2. Data sources

In a developing country like Bangladesh, the analysis of air pollutants, greenhouse gases, and meteorological variables is constrained by the insufficient number of atmospheric monitoring stations, which hampers field measurements. As a result, this study leverages satellite-based data from diverse sources, allowing for a more comprehensive assessment of these critical environmental factors. Detailed information on the data sources can be found in Table 1. The concentrations of four air pollutants (NO_2, SO_2, CO, and O_3) and the greenhouse gas CH_4, provided by the European Space Agency's Sentinel-5 Precursor TROPOMI mission [50]. It is a passive hyperspectral nadir-viewing imager aboard the Sentinel-5 precursor satellite and has been operational since July 2018 [51]. It provides calibrated and near-real-time data from its nadir-viewing spectrometer, which can be utilized to assess air quality variables such as formaldehyde, aerosols, CO, NO_2, and SO_2 [52]. Studies by Griffin et al. [53] and Lorente et al. [54] have demonstrated that TROPOMI's measurements correlate well with actual ground measurements and crowd-sourced air quality data. Additionally, land surface temperature data is sourced from Moderate Resolution Imaging Spectroradiometer (MODIS) details presented in Table 1. The MODIS Terra and Aqua satellites offer nighttime and daytime LST maps and charts with a daily temporal resolution and a spatial resolution of 1 km. All data were accessed via the Google Earth Engine (GEE) platform where pixels containing clouds were excluded.

Annual CO_2 data, available from 1990 to 2021, was sourced from the International Energy Agency (IEA). This organization offers authoritative analysis, comprehensive data, policy recommendations, and solutions to ensure energy security and facilitate the global transition to clean energy. Other pollutants such as $PM_{2.5}$, AOD, and AOT were obtained from NASA Giovanni. NASA Giovanni is an innovative online web tool developed by NASA to help researchers and the public explore and understand Earth science data. It's user-friendly and doesn't require special software, allowing easy access to a wide range of datasets. Giovanni's features include generating plots, maps, and animations, making complex data easier to grasp. It's valuable for studying climate, monitoring the environment, and validating satellite observations. Some previous studies by Prados et al. [55] explored Visualization and Interoperability of Air Quality, while Acker et al. [56] and Acker et al. [57] investigated Public Health and Weather Connections using NASA Giovanni data.
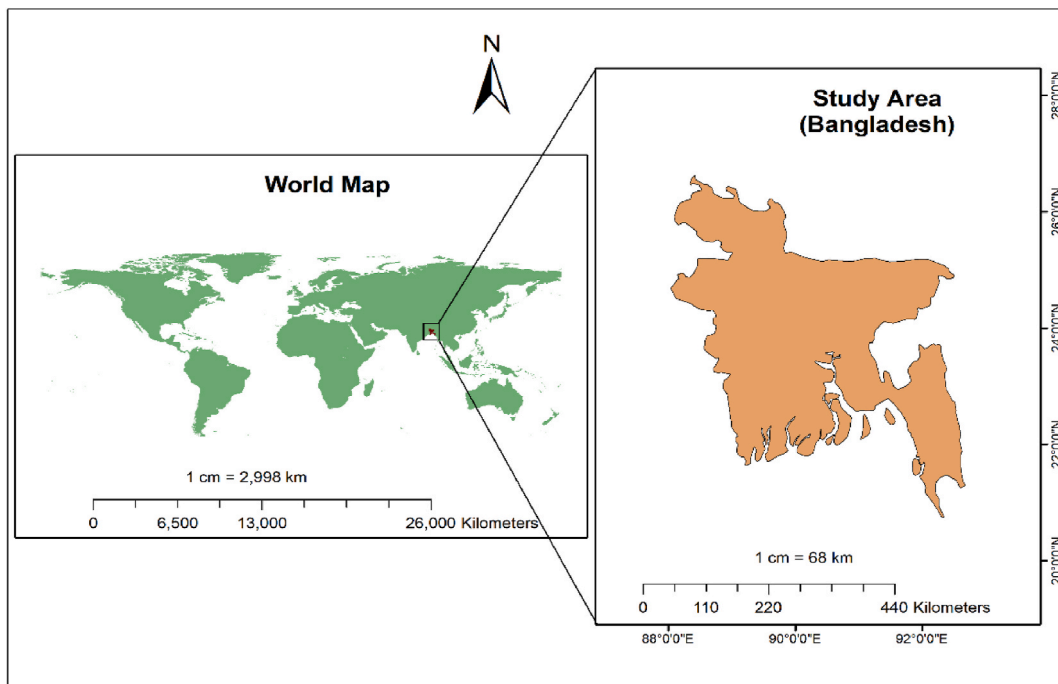

Fig. 1. Geographic location of study area (Bangladesh).

Table 1
Data Sources of different variables.

Parameter	Dataset Provider	Data Availability	Satellites	Dataset/Link	Resolution
NO_2	ESA/ Copernicus	Jul-2018 to Aug-2024	S5P	COPERNICUS/S5P/NRTI/L3_NO$_2$	1113.2 m
SO_2	ESA/ Copernicus	Nov-2018 to Aug-2024	S5P	COPERNICUS/S5P/NRTI/L3_SO$_2$	1113.2 m
CO	ESA/ Copernicus	Nov-2018 to Aug-2024	S5P	COPERNICUS/S5P/NRTI/L3_CO	1113.2 m
O_3	ESA/ Copernicus	Nov-2018 to Aug-2024	S5P	COPERNICUS/S5P/OFFL/L3_O$_3$	1113.2 m
CH_4	ESA/ Copernicus	Feb-2019 to Aug-2024	S5P	COPERNICUS/S5P/OFFL/L3_CH$_4$	1113.2 m
LST	NASA LP DAAC	Feb-2000 to Aug-2024	MODIS	MODIS/061/MOD11A1	1000 m
CO_2	International Energy Agency (IEA)	1990 to 2021		Htt ps://ww w.iea.org/data-and-statistics/data-tools/energy-statistics-data-browser? country=BANGLADESH&fuel=CO220emissions&indicator=CO2BySource	
$PM_{2.5}$	NASA Giovanni	Jan-1980 to Aug-2024	MERRA-2 Reanalysis	https://giovanni.gsfc.nasa.gov/giovanni/ #service=TmAvMp&starttime=&endtime=&dataKeyword=PM2.5	0.625^0
AOD	NASA Giovanni	Oct-2004 to Aug-2024	OMI	https://giovanni.gsfc.nasa.gov/giovanni/ #service=TmAvMp&starttime=&endtime=&dataKeyword=AOD	0.25^0

The monthly and yearly mean data for relative humidity and Sky Surface Albedo were sourced from NASA Power Access Viewer (https://power.larc.nasa.gov/data-access-viewer/). It is a sophisticated online tool that helps users retrieve and visualize meteorological and solar data developed by NASA's POWER project, it supports climate research, renewable energy, and environmental monitoring by offering access to diverse datasets on surface meteorology and solar energy. Users can easily customize and download data on temperature, wind speed, precipitation, and solar radiation. Leonardo et al. [58] compared data from it with field measurements and found a satisfactory level of accuracy.

2.3. Data analysis

This study conducted a comprehensive GIS-based assessment alongside Principal Component Analysis (PCA) using MATLAB to explore the interrelationships among pollutants, greenhouse gases, and meteorological variables. GIS-based approach has been successfully applied in various regions worldwide, examining different air pollutants and meteorological conditions [59–61]. Data and imagery were extracted from multiple datasets, and GIS techniques facilitated detailed image evaluation, while PCA provided insights into the underlying correlations among the variables analyzed.

3. Results

This study considered three types of atmospheric variables: air pollutants, greenhouse gases, and meteorological variables. The results for each category are presented sequentially below. Table 2 and Fig. 2 (a) and (b) represented the year-wise concentrations of observed atmospheric variables in Bangladesh, highlighting their changes before (2019), during (2020), and after the lockdown (2021–2023).

Table 2
Yearly mean data of air pollutants, greenhouse gases, and meteorological variables from different sources.

| Parameters	Year				
	2019	2020	2021	2022	2023
Nitrogen Dioxide/NO_2 (ng/m^3)	0.078	0.076	0.091	0.084	0.086
Sulfur Dioxide/SO_2 (ng/m^3)	0.06	0.05	0.074	0.076	0.09
Carbon monoxide/CO (ug/m^3)	0.043	0.042	0.043	0.041	0.042
Ozone/O_3 (ug/m^3)	0.118	0.121	0.122	0.124	0.122
Particulate Matter less than 2.5 μg/$PM_{2.5}$ (ug/m^3)	40.82	39.97	44.19	40.99	–
Aerosol Optical Depth/AOD	0.64	0.622	0.693	0.687	0.748
Aerosol Optical Thickness/AOT	0.615	0.606	0.665	0.668	0.712
Carbon Dioxide/CO_2 (mol/mol dry air)	0.00041	0.00041	0.00042	–	–
Methane/CH_4 (ug/m^3)	1886.3	1902.15	1915.94	1919.77	1945.29
Land Surface Temperature/LST (^{0}C)	27.13	26.97	27.23	27.64	–
Surface Albedo	0.095	0.094	0.099	0.088	0.092
Relative Humidity/RH (%)	71.83	76.41	71.51	73.96	72.13
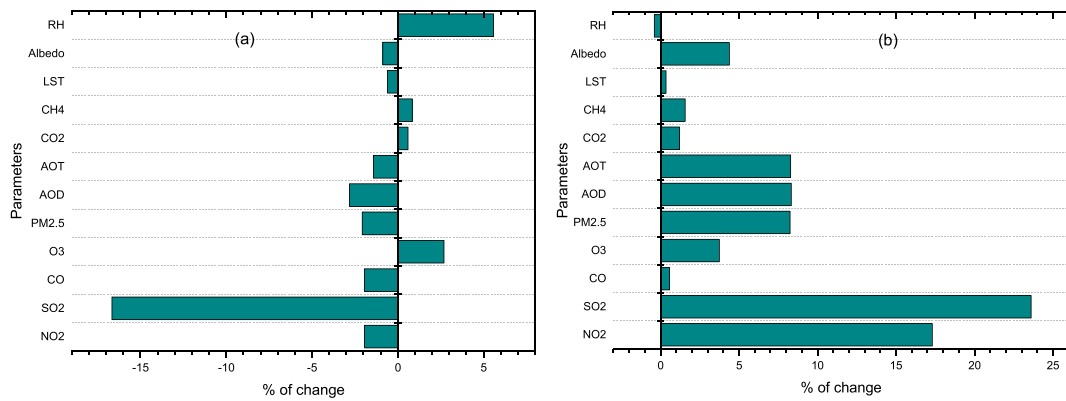
Fig. 2. The changes of all observed variables compared to 2019 in the year (a) 2020 and (b) 2021.

3.1. Air pollutants

This study reveals a fluctuating trend in air pollutants such as NO₂, SO₂, CO, and $PM_{2.5}$ from 2019 to 2023. Fig. 3(a) illustrates NO₂ concentration data, further detailed by the graphical representation in Fig. 4. Results showed a 1.94 % drop in NO₂ levels in 2020 compared to 2019, likely due to reduced activity during the COVID-19 pandemic. However, this decline was short-lived, with NO₂ levels rising sharply by 19.63 % in 2021. In 2022 and 2023, concentrations slightly decreased but remained elevated compared to pre-pandemic levels. Seasonal variation is evident, as NO₂ levels typically decreases during winter and surge by 20–25 % in summer. A notable finding is that March 2021 recorded the highest NO₂ concentration (0.15 ng/m^3). Fig. 4 also shows that the central region, particularly around the capital city, consistently exhibited high NO₂ concentrations (0.1–0.12 µg/m^3), with the affected area expanding significantly post-pandemic.

Similarly, significant changes were observed in SO₂ (sulfur dioxide) concentrations, as shown in Fig. 3(b), with graphical details in Fig. 5. In 2020, during the restricted year, SO₂ levels dropped by 16.67 % compared to 2019. However, by 2021, SO₂ concentrations surged dramatically, rising 48.33 % from 2020 to 23.61 % from 2019. This upward trend continued in subsequent years, with SO₂ levels increasing by 2.5 % in 2022 and a further 18.5 % in 2023 relative to 2021. Fig. 5 reveals that the eastern region of the country experienced higher SO₂ concentrations compared to the west, with post-lockdown years showing a noticeable increase in emissions around the capital city.

The observed trends in CO concentrations from 2019 to 2023, as illustrated in Figs. 6(a) and 7, highlight the substantial impact of human activities on air quality. In 2020, CO levels fell by 1.95 % compared to 2019; however, as restrictions were lifted in 2021, CO concentrations rose by 2.6 %. This upward trend persisted, with a 1.8 % increase in 2023, despite a temporary decrease of 3.9 % in 2022. Seasonally, CO levels typically peaked between March and May, which are known as the extremely hot months following winter in Bangladesh. Notably, observations indicate that CO concentrations are approximately 43 % higher in the immediate post-winter period than during the rainy season.

The annual mean $PM_{2.5}$ concentrations further underscore the impact of lockdown and subsequent activities on air quality, as presented in Fig. 6(b). In 2020, the annual mean $PM_{2.5}$ concentration dropped by approximately 2.03 % compared to 2019. However, this trend reversed in 2021, with PM₂0.5 levels rising by 10.6 %, followed by a 2.5 % increase in 2022 compared to 2020. Seasonal patterns revealed lower $PM_{2.5}$ concentrations from late March through early September, while higher levels were recorded from
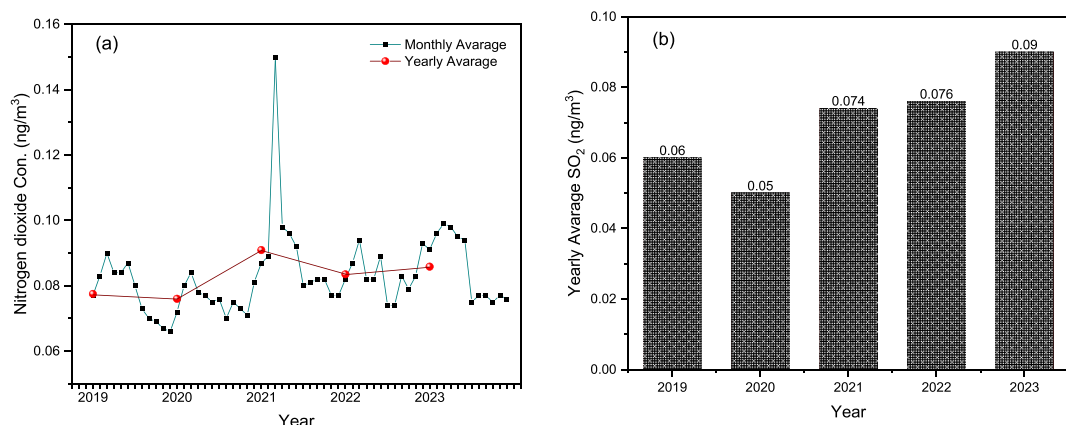

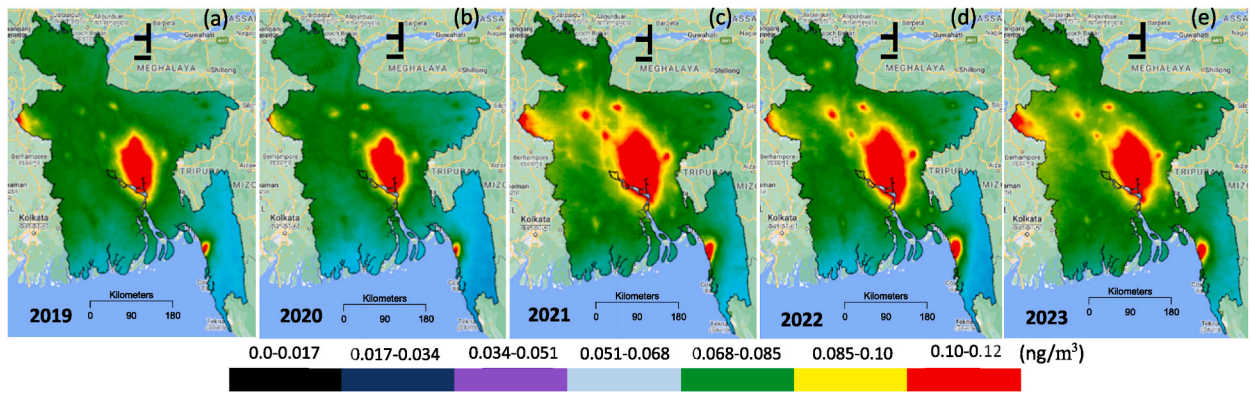**Fig. 3.** (a) Monthly and yearly mean NO_2 Concentrations and (b)yearly mean SO_2 Concentrations.

Fig. 4. NO₂ Concentration Across Bangladesh: Panels (a)–(e) illustrate the concentrations for the years 2019 through 2023, respectively.
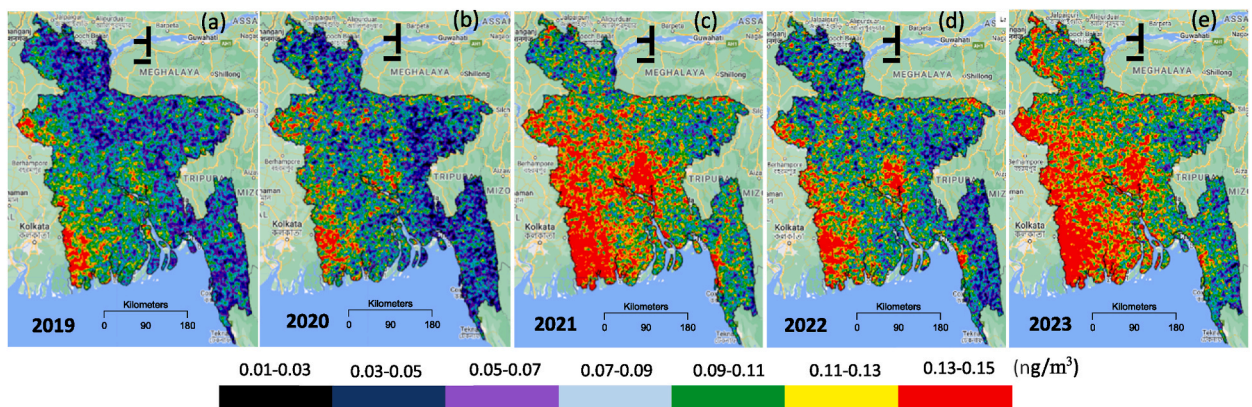

Fig. 5. SO$_2$ Concentration Across Bangladesh: Panels (a)–(e) illustrate the concentrations for the years 2019 through 2023, respectively.
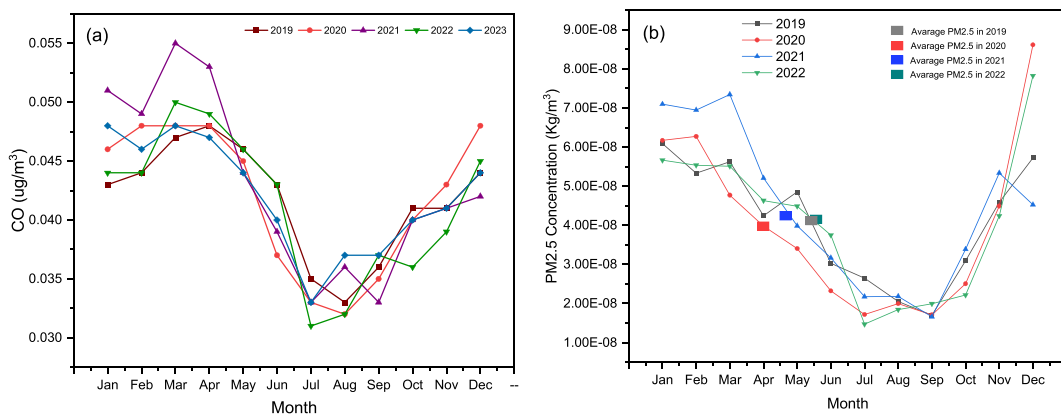

Fig. 6. Monthly and yearly mean Concentrations of (a) CO and (b) PM$_{2.5}$.

November to February, corresponding with the dry winter season. Notably, the results indicate that winter concentrations are consistently nearly 50 % higher than those observed during the rainy season each year.

3.2. Greenhouse gases

This study analyzed the total and per capita CO$_2$ emissions from fossil fuel combustion in Bangladesh shown in Fig. 8(a), focusing on three critical periods: pre-lockdown (2012–2019), during lockdown (2020), and post-lockdown (2021). In 2019, total CO$_2$
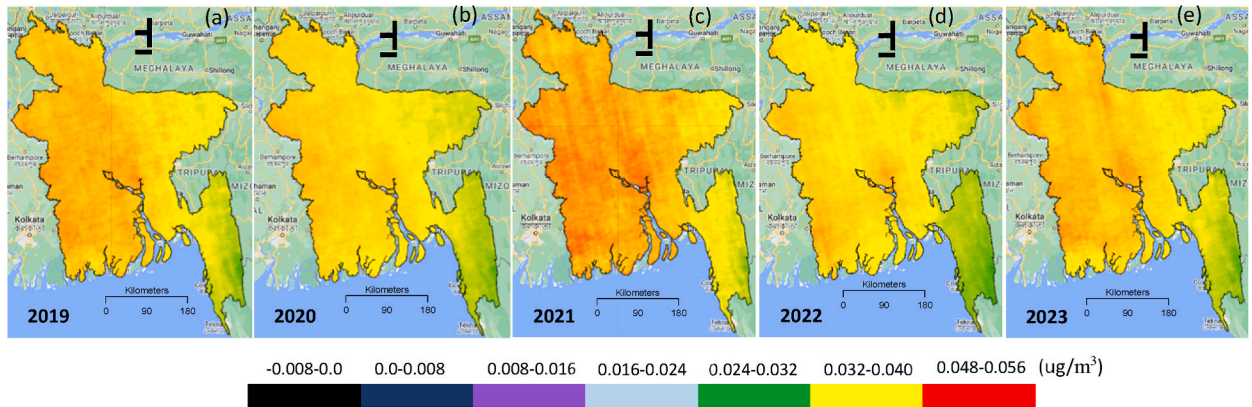
Fig. 7. CO Concentration Across Bangladesh: Panels (a)–(e) illustrate the concentrations for the years 2019 through 2023, respectively.
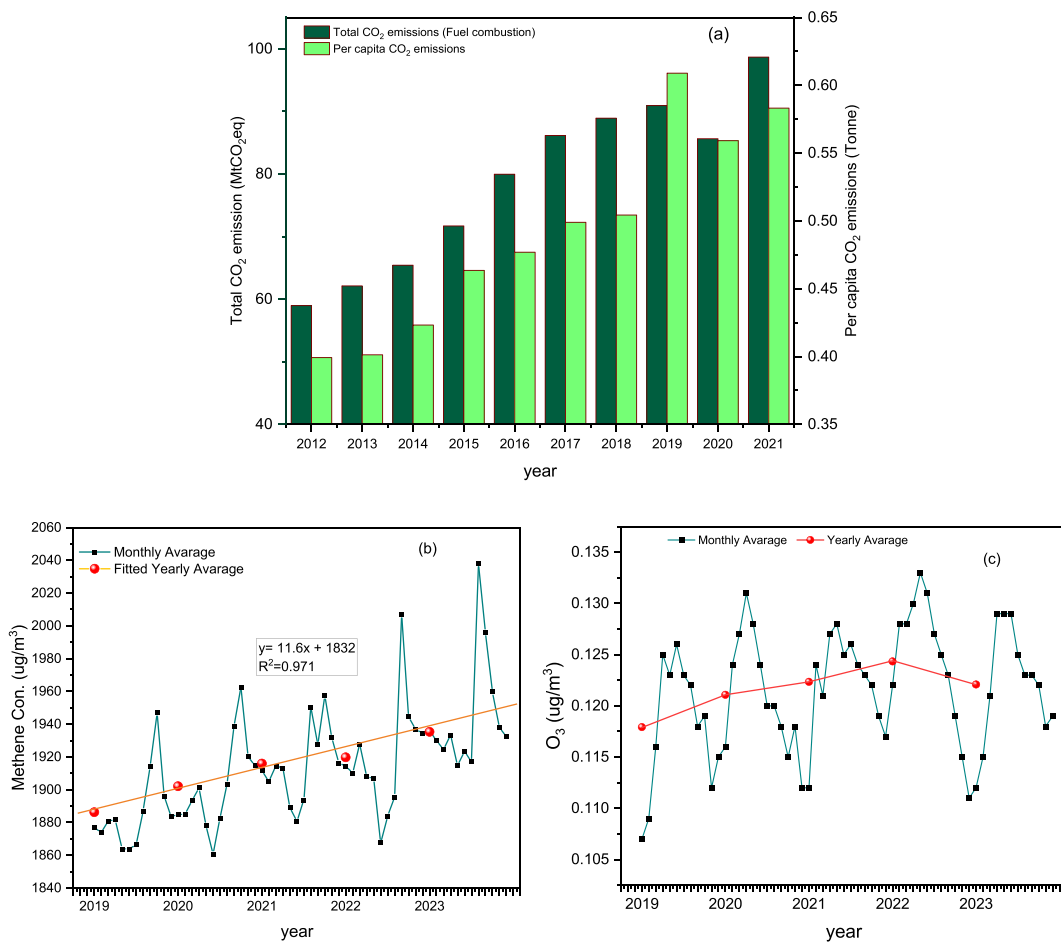

Fig. 8. (a) Total and per capita CO_2 emissions from 2012 to 2021; Monthly and yearly mean Concentrations of (b) CH_4 and (c) O_3.

emissions reached 90.9 Mt, marking a 2 % increase from 2018. During the lockdown in 2020, emissions decreased to 85.6 Mt, representing a 6 % reduction from 2019 concentrations. However, in 2021, emissions surged to 99 Mt, an 8.5 % increase from 2019 and a 15.3 % rise compared to 2020. This figure clearly stated that CO_2 emission is highly proportional to the year in Bangladesh without covid'19 restricted year, 2020.

In contrast, CH_4 concentrations remained unaffected by the lockdown, displaying a steady annual increase of approximately 1 % $\pm$ 0.5 % shown in Fig. 8(b), with the most pronounced rise observed in 2023 presented in Fig. 9. A very nice linear correlation of CH_4
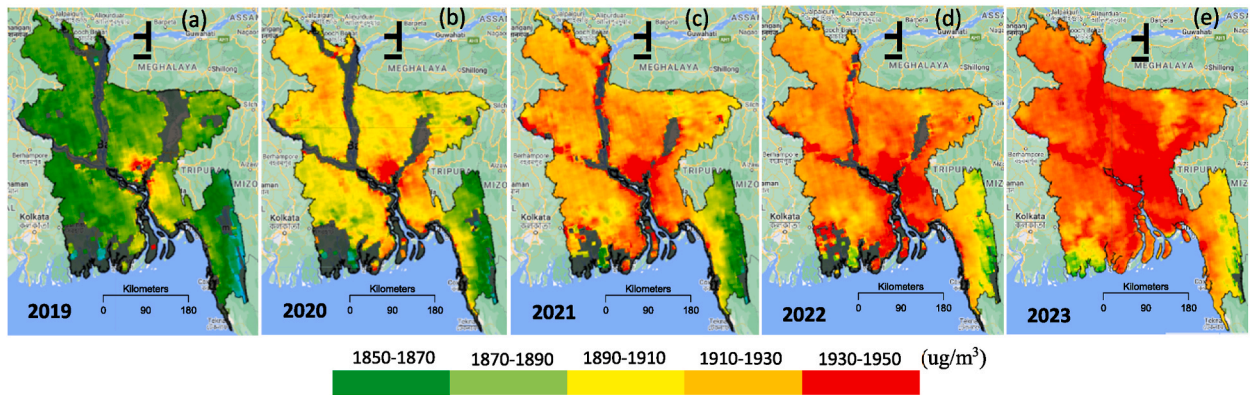
Fig. 9. CH$_4$ Concentration Across Bangladesh: Panels (a)–(e) illustrate the concentrations for the years 2019 through 2023, respectively.

concentration with time observed in this figure where correlation coefficient, R^2 is 0.971, slope 11.6 μg/m^3. y and intersect 1832 μg/m^3. In last 5-year years observation indicates that methane concentration increases almost 120 μg/m^3 that almost 7 % increase from 2019 to 2023. Observations also indicate that the central region of the country is more adversely affected than other areas.m^3

There was a significant change in O$_3$ concentration across Bangladesh from 2019 to 2023, demonstrating a continuous upward trend from 2020 to 2022, as illustrated in Fig. 8(c). Specifically, O$_3$ concentrations increased by 2.7 % in 2020, followed by a 1 % rise in 2021, and a further increase of 1.6 % in 2022. However, in 2023, a decline of 1.8 % was observed. Notably, the lowest increase in O$_3$ concentrations occurred in 2021, during the post-lockdown period, as depicted in Fig. 10. This figure also indicates that changes in O$_3$ concentrations were relatively slow in response to COVID-19 restrictions. Additionally, it highlights that the northern regions of the country exhibited higher O$_3$ concentrations throughout the observed years.

3.3. Meteorological variables

Relative humidity (RH) is a key factor influencing both atmospheric chemistry and the physical state of air pollutants. The lock-down period significantly impacted RH levels. This research indicated a notable increase in RH during 2020, as illustrated in Fig. 11(a), where values reached 76 %, reflecting a 6.4 % rise from 2019. Changes in the observed variables across three different years are depicted in Fig. 2(a) and (b). By 2021, RH levels returned to those seen in 2019. In the following two years (2022 and 2023), RH remained relatively stable, exhibiting only a slight fluctuation of 1–2% compared to the years 2019 and 2021. Additionally, the data suggests a significant increase in RH during the rainy season, reaching nearly 80 %, in contrast to the lower levels observed during winter, which are around 45 %.

This study examined LST across the country through two observation methods: monthly and annual LST for the entire year, as well as daily and monthly LST during the winter and summer seasons, as illustrated in Fig. 11(b). The findings indicated that the average yearly LST in 2020 decreases by 0.164 °C compared to 2019 shown in Fig. 12. In 2021, there was subsequent increases of 0.26 °C. However, in 2022, LST fell by 0.42 °C, with 2022 recording the lowest temperatures and 2021 the highest. Seasonal analysis revealed that 2021 marked the peak temperatures in both winter and summer, with averages of 24.08 °C and 30.14 °C, respectively. Conversely, the lowest winter and summer temperatures were recorded in 2020 and 2023, measuring 23.51 °C and 27.61 °C, respectively. Notably, the largest temperature difference between summer and winter occurred in 2021, at 6.06 °C, while the smallest difference was 3.87 °C
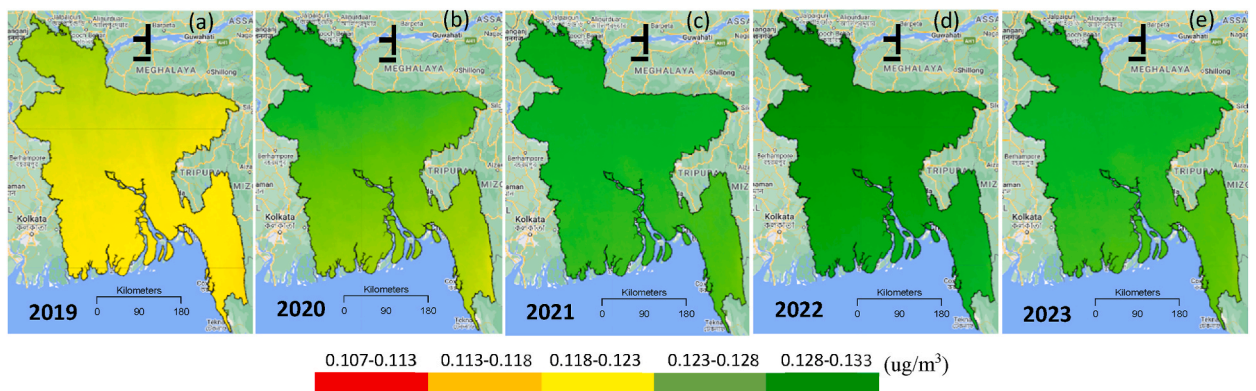

Fig. 10. O$_3$ Concentration Across Bangladesh: Panels (a)–(e) illustrate the concentrations for the years 2019 through 2023, respectively.
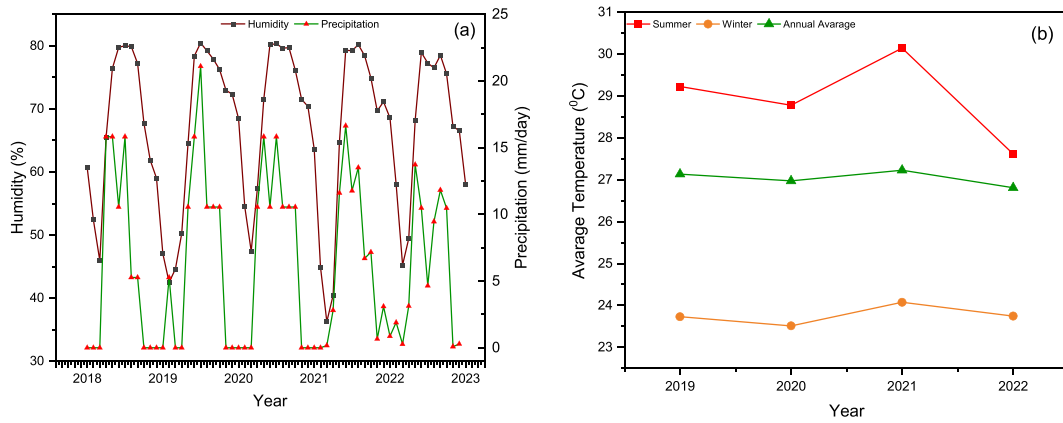
Fig. 11. (a) Monthly Relative Humidity and precipitation and (b) Seasonal land surface temperature.
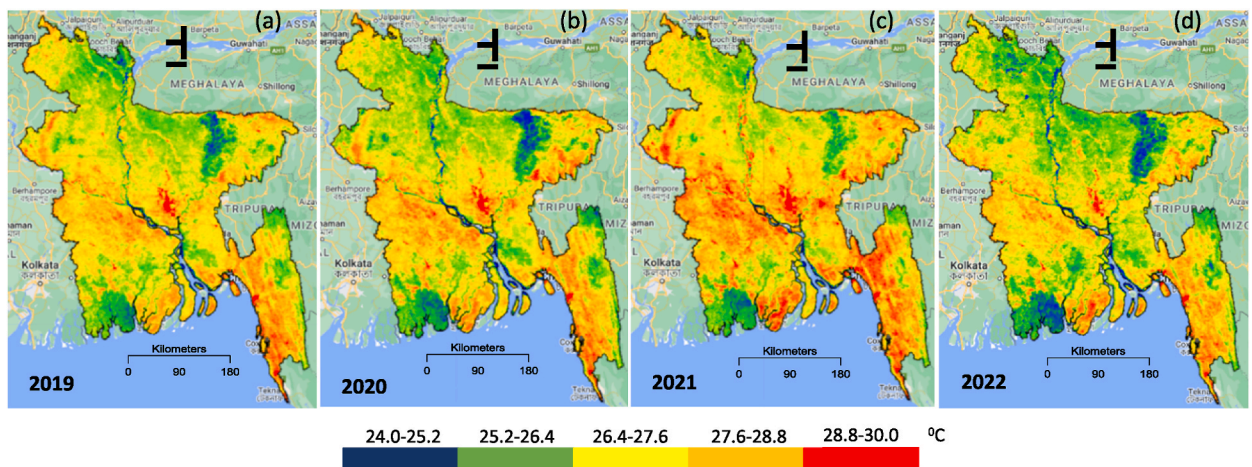

Fig. 12. Land Surface Temperature Across Bangladesh: Panels (a)–(d) illustrate the LST for the years 2019 through 2022, respectively.

in 2023.

Our study area demonstrated significant variations in albedo over the five-year period, consistent with established principles. In 2020, albedo decreased by 0.9 % compared to 2019, likely attributed to reduced human activity during the COVID-19 lockdown, as shown in Fig. 13(a). In 2021, however, albedo increases markedly by 5.6 % relative to 2020. This trend reversed in 2022, when albedo
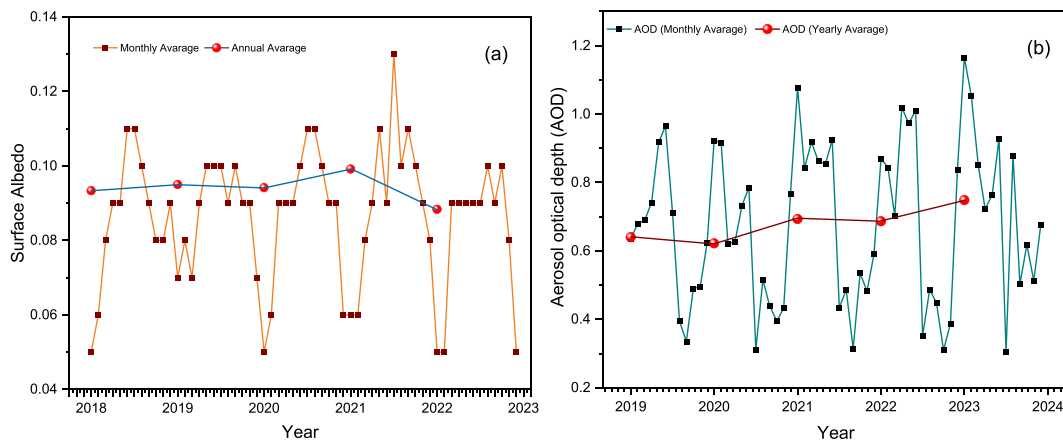

Fig. 13. Monthly and yearly mean (a) Albedo and (b) AOD.

experienced a substantial decline of nearly 11 % from the previous year. In 2023, there was a recovery with an increase of 4 % in albedo compared to 2022. Seasonal observations revealed that during the rainy season, from July to September, albedo values rose, while during the winter season, from December to February, it consistently dropped significantly almost every year.

Our study's examination of Aerosol Optical Depth (AOD) from 2019 to 2023 reveals significant trends that are essential for understanding the effects of various environmental and anthropogenic factors, as depicted in Fig. 13(b). The results indicates that 2020, a year characterized by global lockdowns due to the COVID-19 pandemic, saw only a marginal decrease in AOD compared to 2019, with a reduction of just 2.8 %.

In 2021, there was a significant increase in AOD, rising by 11.5 % compared to the previous year. The highest AOD recorded during our study period reached 0.748 $\mu g/cm^3$ in 2023, reflecting a steady annual increase in aerosol concentrations, with the exception of the anomaly in 2020. Additionally, the lowest AOD concentrations were consistently observed during July and August each year, attributed to the rainy season.

4. Discussion

Air pollutants such as NO_2, SO_2, $PM_{2.5}$, and CO primarily originate from motor vehicles (due to fossil fuel combustion), wood combustion, biomass burning, small businesses using combustion techniques, and industrial activities like brick kilns reported by Sariful et al. [21]. Some previous studies [40,62–66] conducted in various regions worldwide have found significant changes in air pollutant concentrations when comparing the days immediately before and during the COVID-19 lockdown period.

The reduction in the concentration of NO_2 and SO_2 in restricted year associated due reductions in industrial activities and vehicular emissions that is also conducted by Wang et al. [67]. The following of the restricted year (2021), a significant rise in concentration possibly due to the resumption of economic activities and increased industrial output post-lockdown [68,69]. In the next two year (2022 and 2023), concentration dropped from 2021 but continuously rise with respect to 2019. This variability may be attributed to intermittent policy measures, industrial activity changes, and the meteorological conditions average [70,71].

This seasonal trend contradicts findings from previous studies, such as those by Masiol et al. [72] and Squizzato et al. [73], which reported higher NO_2 concentrations during winter months due to lower atmospheric dispersion and increased heating. This peak could be associated with specific events or activities during that period, such as industrial operations, agricultural burning, or meteorological conditions that favored the accumulation of pollutants [74,75]. Monthly observations indicate a significant drop in SO_2 concentrations from June to October (Rainy season) each year. This seasonal decline is likely due to the scavenging effect of monsoon rains, which effectively remove SO_2 from the atmosphere [72,73].

CO is a harmful air pollutant primarily Produced by incomplete combustion of carbon-based fuels. In 2020, its decrement observed likely due to the stringent lockdown measures that significantly curtailed transportation and industrial activities, leading to reduced fossil fuel combustion, a primary source of CO emissions [76,77]. However, in 2021, as restrictions eased and economic activities resumed, CO concentrations increased significantly from past two years. And continues increase in the following years observed due to industrial and agricultural activities those burn the larger amount of fossil fuel. This fluctuation underscores the impact of resuming economic activities on air quality [64]. Seasonally, CO concentrations peaked between February and April each year, correlating with increased vehicular emissions and agricultural burning post-harvest which is conducted by Venter et al. [52]. Menut et al. [3] found the significant reductions from June to October can be attributed to the monsoon season, which enhances pollutant dispersion.

In 2020, the yearly mean $PM_{2.5}$ concentration decreased compared to 2019, reflecting the immediate impact of reduced industrial output and vehicular traffic during the lockdown [78]. However, in 2021 concentration increased from previous two year and this pattern is also found in previous study [52,79]. In rainy season, less concentration mainly due to the settlement of particulate matter by rain water. In winter, increased use of biomass for heating, and post-harvest agricultural residue burning, increase the overall concentration, consistent with previous studies [80,81].

According to the International Energy Agency [82,83], global CO_2 emissions from fuel combustion surged by almost 6 % in 2021, nearly reaching pre-pandemic concentrations. Fossil fuels dominated the energy supply, accounting for 80 % of the total, with oil at almost 30 %, coal at 27 %, and natural gas at 24 %. Coal was the largest contributor to global emissions at 44 %, followed by oil at 32 % and natural gas at 22 % [International Energy Agency, 2021]. Bangladesh is developing country, here the industrial transportation activities are growing very rapidly those are enhancing CO_2 emission every year. But in 2020 a decrease in CO_2 shows due to decreased industrial activities and transportation those minimized the burning of fossil fuel.

Results show the continuous increase in CH_4. The agricultural sector a significant contributor to methane emissions, was not significantly curtailed during the lockdown, as food production remained a priority. Livestock farming, responsible for enteric fermentation, landfill, and rice paddies, a source of anaerobic decomposition, continued to emit methane at typical rates [84,85].

Additionally, the increased CH_4 concentrations in 2023 could be linked to a rebound in economic activities post-lockdown, with intensified agricultural activities and waste generation contributing to higher emissions [86]. Moreover, natural feedback mechanisms, such as increased temperatures accelerating microbial processes in wetlands, may also play a role in enhancing methane emissions [87].

During the COVID-19 lockdown, transportation and industries slowed down, emissions of pollutants like nitrogen oxides (NOx) dropped. Normally, NOx reacts with other chemicals in the air to form ground-level ozone (O_3). But with less NOx around, the usual chemical reactions in the atmosphere shifted, sometimes causing O_3 levels to rise because there was less NOx available to break it down [72,73]. This trend aligns with previous studies [40,88,89] that observed similar increases in O_3 concentrations during the COVID-19 lockdown.

High RH concentrations can significantly enhance the secondary formation of aerosols, particularly sulfate and nitrate particles, by

providing the necessary water vapor for chemical reactions [90]. Conversely, low RH can lead to the evaporation of water from aerosol particles, reducing their size and potentially decreasing the overall particulate matter (PM) concentration found by Zhang et al. [91]. In the lockdown year, RH increase was likely due to the reduced industrial activity and transportation, which also led to notable reductions in air pollutants and GHGs which are mostly inversely correlated with RH shown in Fig. 14. Our findings show an inverse relationship of RH with most pronounced gases (NO_2 and SO_2) by lockdown, shown in Fig. 14. And the similar observations found by Finlayson-Pitts and Pitts [92] and Seinfeld and Pandis [93].

Pollutants and GHG are linearly correlated with LST that's why may be in 2020 and 2021 the LST shows decreased and increased respectively. RH is another reason may be influenced the LST. Higher RH concentrations in 2020 likely contributed to the formation of secondary aerosols, while the reduction in pollutant emissions during the same period led to a decrease in LST. The subsequent increase in RH in 2021, combined with higher emissions of GHGs and other pollutants as economic activities resumed, resulted in higher LSTs.

Albedo, the measure of the reflectivity of the Earth's surface, is a critical factor influencing local and global climate dynamics by affecting the energy balance and the urban heat island effect [94]. In the lockdown year, the reduction in activity led to decreased dust and particulate matter deposition on surfaces, which maintained relatively higher reflectivity [94,95]. In post lockdown, the sharp decrease may be linked to intensified urbanization and deforestation activities, which replaced reflective natural surfaces with darker, less reflective ones. In 2023, the rise potentially may be due to efforts in reforestation or changes in agricultural practices that increased the reflectivity of the land surface.

The observed average in albedo is closely linked to fluctuations in air pollutant and GHG concentrations. The increase in GHG emissions, particularly carbon dioxide (CO_2) and methane (CH_4), contributes significantly to global warming, which alters weather patterns and subsequently impacts surface albedo studied by Pielke et al. [95]. Furthermore, changes in land use and urbanization, which directly affect albedo, also serve as sources of air pollutants. This directly connects the observed changes in albedo to broader environmental and climatic shifts, highlighting the interconnectedness of human activities, atmospheric composition, and climate dynamics [94].

This minor reduction of AOD in 2020 suggests that despite the substantial reduction in human activities such as industrial operations and vehicular traffic during the lockdown, the overall aerosol load in the atmosphere was not significantly affected. This could be attributed to the persistence of other sources of aerosols such as agricultural activities, natural dust, and biomass burning which continued unabated during the lockdown period. In 2021, the surge can be linked to the resumption of economic activities and industrial operations post-lockdown, highlighting the rebound effect where pollution concentrations tend to spike as restrictions are lifted and activities normalize. This trend aligns with other studies that have observed similar post-lockdown increases in pollution concentrations [52,96]. This rising trend in AOD could be indicative of escalating anthropogenic activities and possibly changes in regional climatic conditions that affect aerosol production and dispersion. And in the rain season, rain enhances the wet deposition processes, thereby cleansing the atmosphere from aerosols [97].

4.1. Correlations among the variables

Fig. 15 presents the correlation coefficients between various atmospheric variables. The results show that, with the exception of O_3, all variables are negatively correlated with relative humidity (RH). The strongest inverse relationship is observed between $PM_{2.5}$ and RH, with a correlation coefficient of −0.674. Additionally, greenhouse gases such as CH_4 and CO_2 exhibit strong positive correlations with SO_2 (0.8736 and 0.938, respectively), LST (0.8196 for CH_4 and 0.8976 for CO_2), and AOD (0.919 for CH_4 and 0.9538 for CO_2). These relationships suggest that greenhouse gases are closely linked to both air pollutants and meteorological factors. Furthermore, NO_2, SO_2, and $PM_{2.5}$ exhibit strong positive correlations with one another, with correlation coefficients of 0.767 between NO_2 and SO_2 and 0.8374 between SO_2 and $PM_{2.5}$. CO, on the other hand, shows a notable negative correlation with O_3 (−0.736) but positive correlations with surface albedo (SAB) (0.9177). O_3, which stands out due to its negative correlation with Surface Albedo (SAB) (−0.486), displays relatively lower correlation values with other pollutants compared to RH. Additionally, aerosol optical thickness
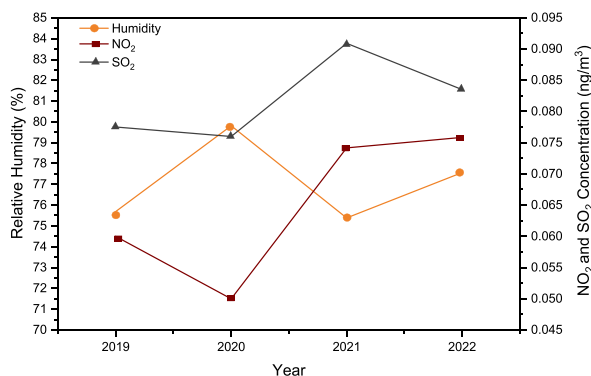

Fig. 14. Relation of RH with NO_2 and SO_2.

	NO2	SO2	CO	O3	PM2.5	AOD	AOT	CO2	CH4	LST	SAB	RH
NO2	1											
SO2	0.767	1										
CO	0.098	-0.232	1									
O3	0.544	0.5326	-0.736	1								
PM2.5	0.821	0.8374	0.229	0.2683	1							
AOD	0.765	0.9875	-0.193	0.5214	0.8911	1						
AOT	0.766	0.9871	-0.284	0.6049	0.8516	0.9944	1					
CO2	0.631	0.938	-0.55	0.7306	0.6557	0.9221	0.9538	1				
CH4	0.631	0.8736	-0.428	0.6965	0.7698	0.919	0.9385	0.9229	1			
LST	0.529	0.9133	-0.568	0.6332	0.5516	0.8681	0.8976	0.9725	0.8196	1		
SAB	0.234	-0.265	0.9177	-0.486	0.2624	-0.197	-0.265	-0.532	-0.326	-0.632	1	
RH	-0.63	-0.587	-0.553	0.206	-0.674	-0.546	-0.482	-0.286	-0.181	-0.333	-0.372	1

Fig. 15. Correlation coefficient from the yearly average data of observed atmospheric variables by Principal Component Analysis (PCA).

(AOT) shows a strong positive correlation with AOD (0.9944), linking it with both particulate matter and meteorological factors.

5. Conclusions

This study used satellite remote sensing to assess the data of different air pollutants, greenhouse gases, and meteorological variables from 2019 to 2023 (pre to post COVID-19 lockdown). GIS and PCA approach adopted to find the patterns, correlations, and trends among the observe variables. The findings reveal that reduced human and industrial activities during the lockdown year significantly lowered emissions, although the extent varied across different sectors and sources. Emissions and LST significantly increased in 2021 compared to 2019 and 2020, and although air quality slightly improved in 2022–2023 from 2021 but did not return to 2019 concentrations. SO_2 exhibited the most notable changes, with a 16.67 % reduction in 2020, followed by $PM_{2.5}$ at 3.1 %. In 2021, SO_2 showed a 23.6 % increase, followed by NO_2 at 17.3 %, relative to pre-lockdown concentrations. CH_4 concentrations were unaffected by the lockdown as its primary sources were not correlated with restrictions. It increased almost 7 % in last 5 years. LST decreased by 0.16 °C in 2020, rose slightly in 2021, and returned to 2019 concentrations in subsequent years. RH increased during the lockdown year due to lower air pollutant concentrations. Seasonal observations indicate that most emissions decrease during the rainy season (June to August) because the rain helps to wash out some of the emission concentrations. The study also highlights those major industrial cities, such as Dhaka, were significant emission-prone areas compared to other regions. An interrelationship was identified between industrial and human activities and all observed variables, as well as a significant link between air pollutants and meteorological factors. Correlation coefficients shows most of the variables are negatively correlated with RH. GHG like CH_4 and CO_2 are strongly correlated with pollutants such as SO_2 and meteorological variables like LST and AOD, indicating that the increase in these gases is closely linked to industrial emissions and temperature changes. Notably, a strong inverse correlation between $PM_{2.5}$ and RH (−0.674) suggests that higher humidity levels can help mitigate particulate matter concentrations. Additionally, air pollutants such as NO_2, SO_2, and $PM_{2.5}$ exhibit strong positive correlations with one another, indicating that industrial and transportation sources contribute significantly to multiple pollutants simultaneously.

CRediT authorship contribution statement

Md. Tushar Ali: Writing – review & editing, Writing – original draft, Validation, Software, Methodology, Investigation, Data curation, Conceptualization. **Islam M. Rafizul:** Supervision, Formal analysis. **Quazi Hamidul Bari:** Visualization, Validation, Supervision, Investigation, Formal analysis.

Recommendations for environmental policymakers

Reducing air pollutants and greenhouse gases in Bangladesh requires enforcing stricter emission standards for industries and vehicles, with a focus on curbing SO_2, NO_2, $PM_{2.5}$, and CO emissions, especially in major industrial city like Dhaka. The promotion of electric vehicles and cleaner technologies in industries will significantly help curb emissions. Additionally, transitioning from fossil fuels to renewable energy sources such as solar and wind can lower the carbon footprint. Implementing energy-efficient technologies and stricter vehicle emission norms will further reduce pollutants. To specifically address methane (CH_4) emissions in Bangladesh, targeted actions should focus on sectors where methane is most prevalent, such as agriculture, waste management, and energy. Policymaker should promote **biogas production** from organic waste and livestock manure, providing a sustainable energy source while reducing methane release into the atmosphere.

While this study effectively captures the temporal changes and correlations in pollutant levels, its primary focus is not on directly

assessing the health impacts of these pollutants. The significant post-lockdown increase in emissions highlights potential health risks, especially from pollutants like SO_2, NO_2, and $PM_{2.5}$, which are well-documented for their harmful effects. However, to fully understand the health implications in Bangladesh, more comprehensive epidemiological studies would be needed, incorporating in situ air quality data alongside health records from the population. This study provides valuable insights into pollution trends, but further research is essential to quantify their direct impact on human health.

Data and code availability

Data and code will be made available on request.

Funding sources

Declaration of competing interest

The authors declare that they have no known competing financial interests or personal relationships that could have appeared to influence the work reported in this paper.

Acknowledgements

References

[1] WHO, Coronavirus disease 2019 (COVID-19): situation report—1, World Health Organization, Geneva, https://www.who.int/docs/default-source/coronaviruse/situation-reports/20200121-sitrep-1-2019-ncov.pdf?sfvrsn=20a99c10_4, 2020. Accessed: Jun. 11, (2020).

[2] L. Martelletti, P. Martelletti, Air pollution and the novel COVID-19 disease: a putative disease risk factor, SN Compr, Clin. Med. 2 (2020) 383–387, https://doi.org/10.1007/s42399-020-00274-4.

[3] L. Menut, B. Bessagnet, G. Siour, S. Mailler, R. Pennel, A. Cholakian, Impact of lockdown measures to combat COVID-19 on air quality over western Europe, Sci. Total Environ. 741 (2020) 140426, https://doi.org/10.1016/j.scitotenv.2020.140426.

[4] WHO, Coronavirus disease 2019 (COVID-19): situation report—51, World Health Organization, Geneva, https://www.who.int/docs/default-source/coronaviruse/situationreports/20200311-sitrep-51-covid-19.pdf, 2020. Accessed: Jun. 11, (2020).

[5] Worldometer, COVID-19 coronavirus pandemic, Available: https://www.worldometers.info/coronavirus/, 2024.

[6] Worldometer, Annual population data of Bangladesh, Available: https://www.worldometers.info/world-population/bangladesh-population/, 2024.

[7] IPCC, Changes in Atmospheric Constituents and in Radiative Forcing, Fourth Assessment Report, Cambridge University Press, 2007.

[8] A.M. Van Tienhoven, M.C. Scholes, Air pollution impacts on vegetation in South Africa, in: Air Pollution Impacts on Crops and Forests: A Global Assessment, Imperial College Press, London, 2003, pp. 237–262.

[9] WHO, Air Quality Guidelines: Global Update, Particulate Matter, Ozone, Nitrogen Dioxide, and Sulfur Dioxide, World Health Organization, 2005, 2006.

[10] S. Dogan, C. Kilicoglu, H. Akinci, H. Sevik, M. Cetin, N. Kocan, Comprehensive risk assessment for identifying suitable residential zones in Manavgat, Mediterranean Region, Eval. Progr. Plann. 106 (2024) 102465, https://doi.org/10.1016/j.evalprogplan.2024.102465.

[11] M. Cetin, Climate comfort depending on different altitudes and land use in the urban areas in Kahramanmaras City, Air Quality, Atmosphere & Health 13 (2020) 991–999, https://doi.org/10.1007/s11869-020-00858-y.

[12] M. Cetin, The effect of urban planning on urban formations determining bioclimatic comfort area's effect using satellite images on air quality: a case study of Bursa city, Air Quality, Atmosphere & Health 12 (2019) 1237–1249, https://doi.org/10.1007/s11869-019-00742-4.

[13] Y. Zhao, et al., Substantial changes in nitrogen dioxide and ozone after excluding meteorological impacts during the COVID-19 outbreak in mainland China, Environ. Sci. Technol. Lett. 7 (6) (2020) 402–408, https://doi.org/10.1021/acs.estlett.0c00605.

[14] X. Huang, et al., Enhanced secondary pollution offset reduction of primary emissions during COVID-19 lockdown in China, Natl. Sci. Rev. (2020), https://doi.org/10.1093/nsr/nwaa137.

[15] T. Le, et al., Unexpected air pollution with marked emission reductions during the COVID-19 outbreak in China, Science 369 (2020) 702, https://doi.org/10.1126/science.abd4049.

[16] A.P. Yunus, Y. Masago, Y. Hijioka, COVID-19 and surface water quality: improved lake water quality during the lockdown, Sci. Total Environ. 731 (2020) 139012, https://doi.org/10.1016/j.scitotenv.2020.139012.

[17] J. Kim, et al., New era of air quality monitoring from space: geostationary environment monitoring spectrometer (GEMS), Bull. Am. Meteorol. Soc. 101 (2020) E1–E22, https://doi.org/10.1175/BAMS-D-18-0013.1.

[18] S. Saadat, D. Rawtani, C.M. Hussain, Environmental perspective of COVID-19, Sci. Total Environ. 728 (2020) 138870, https://doi.org/10.1016/j.scitotenv.2020.138870.

[19] B. Anderson, K.A. Dirks, Preliminary analysis of changes in outdoor air quality in the City of Southampton during the 2020 COVID-19 outbreak to date: a response to DEFRA's Call for Evidence 1 on Estimation of changes in air pollution emissions, concentrations and exposure during the COVID-19 outbreak in the UK, Available: http://eprints.soton.ac.uk/id/eprint/439813, 2020.

[20] S. Chaudhary, S. Kumar, R. Antil, S. Yadav, Air quality before and after COVID-19 lockdown phases around New Delhi, India, J. Health & Pollution 11 (30) (2021) 1–11.

[21] C. Jephcote, A.L. Hansell, K. Adams, J. Gulliver, Changes in air quality during COVID-19 'lockdown' in the United Kingdom, Environ. Pollut. (2020), https://doi.org/10.1016/j.envpol.2020.116011.

[22] Y. Wang, et al., Four-month changes in air quality during and after the COVID-19 lockdown in six megacities in China, Environ. Sci. Technol. Lett. 7 (11) (2020) 802–808, https://doi.org/10.1021/acs.estlett.0c00605.

[23] M. Sarmadi, S. Rahimi, M. Rezaei, D. Sanaei, M. Dianatinasab, Air quality index variation before and after the onset of COVID-19 pandemic: a comprehensive study on 87 capital, industrial and polluted cities of the world, Environ. Sci. Eur. 33 (2021) 134, https://doi.org/10.1186/s12302-021-00575-y.

[24] G. Manoli, et al., Magnitude of urban heat islands largely explained by climate and population, Nature 573 (2019) 55–60, https://doi.org/10.1038/s41586-019-1512-9.

[25] S. Peng, et al., Surface urban heat island across 419 global big cities, Environ. Sci. Technol. 46 (2012) 696–703, https://doi.org/10.1021/es2030438.

[26] M.T. Ali, M.H. Rashid, The effects of coarser sand addition on thermal properties of pervious concrete, Innovative Infrastructure Solutions 9 (402) (2024), https://doi.org/10.1007/s41062-024-01711-2.

[27] X. Yang, et al., Contribution of urbanization to the increase of extreme heat events in an urban agglomeration in east China, Geophys. Res. Lett. 44 (2017) 6940–6950, https://doi.org/10.1002/2017gl074084.

[28] G. Roshan, R. Sarli, S.W. Grab, The case of Tehran's urban heat island, Iran: impacts of urban "lockdown" associated with the COVID-19 pandemic, Sustain. Cities Soc. 75 (2021) 103263, https://doi.org/10.1016/j.scs.2021.103263.

[29] S. Mukherjee, A. Debnath, Correlation between land surface temperature and urban heat island with COVID-19 in New Delhi, India, Research Square (2020), https://doi.org/10.21203/rs.3.rs-30416/v1. Available:.

[30] A.M. Kenawy, et al., The impact of COVID-19 lockdowns on surface urban heat island changes and air-quality improvements across 21 major cities in the Middle East, Environ. Pollut. 288 (2021) 1–12, https://doi.org/10.1016/j.envpol.2021.117802. Available:.

[31] M. Cetin, M. Ozenen Kavlak, M.A. Senyel Kurkcuoglu, G. Bilge Ozturk, S.N. Cabuk, A. Cabuk, Determination of land surface temperature and urban heat island effects with remote sensing capabilities: the case of Kayseri, Türkiye, Nat. Hazards 120 (6) (2024) 5509–5536, https://doi.org/10.1007/s11069-024-06431-5.

[32] Z. Liu, et al., Urban heat islands significantly reduced by COVID-19 lockdown, Geophys. Res. Lett. 49 (2022) e2021GL096842, https://doi.org/10.1029/2021GL096842.

[33] Z. Cetin, I. Varol, H.B. Ozel, H. Sevik, The effects of climate on land use/cover: a case study in Turkey by using remote sensing data, Environ. Sci. Pollut. Control Ser. 30 (3) (2023) 5688–5699, https://doi.org/10.1007/s11356-022-22566-z.

[34] Z. Cetin, I. Varol, H.B. Ozel, A geographic information systems and remote sensing–based approach to assess urban micro-climate change and its impact on human health in Bartin, Turkey, Environ. Monit. Assess. 195 (2023), https://doi.org/10.1007/s10661-023-11105-z. Art. no. 540.

[35] Ghaffar Ali, et al., Environmental impacts of shifts in energy, emissions, and urban heat island during the COVID-19 lockdown across Pakistan, J. Clean. Prod. 291 (2021) 1–12, https://doi.org/10.1016/j.jclepro.2021.125806. Available:.

[36] GDP, savings and investment, Chapter 2), Bangladesh Economic Review (BER), Ministry of Finance, Government of the People's Republic of Bangladesh, Bangladesh, 2019, p. 19.

[37] B.A. Begum, S.K. Biswas, P.K. Hopke, Assessment of trends and present ambient concentrations of PM3.2 and PM10 in Dhaka, Bangladesh, Air Quality, Atmosphere & Health 1 (2008) 125–133, https://doi.org/10.1007/s11869-008-0018-7. Available:.

[38] M. Shammi, et al., Strategic assessment of COVID 19 pandemic in Bangladesh: comparative lockdown scenario analysis, public perception, and management for sustainability, Environ. Dev. Sustain. 23 (2021) 6148–6191, https://doi.org/10.1007/s10668-020-00867-y. Available:.

[39] Declining infection rate drives hopes of curbing COVID spread in Bangladesh, bdnews24.com, 1 February, Available: https://www.bdnews24.com, 2021.

[40] M.S. Islam, et al., Impacts of nationwide lockdown due to COVID-19 outbreak on air quality in Bangladesh: a spatiotemporal analysis, Air Quality, Atmosphere & Health 14 (2021) 351–363, https://doi.org/10.1007/s11869-020-00940-5. Available:.

[41] S. Begum, Sustainable urban transportation: performance indicators and some analytical approaches, J. Urban Plann. Dev. 134 (1) (2008) 43–56, https://doi.org/10.1061/(ASCE)0733-9488(2008)134:1(43. Available:.

[42] S.A.I. Mahmood, Air pollution kills 15,000 Bangladeshis each year: the role of public administration and governments integrity, J. Publ. Adm. Pol. Res. 3 (2011) 129–140, https://doi.org/10.5897/JPAPR.9000004. Available:.

[43] WHO, WHO global urban ambient air pollution database (update 2016), World Health Organization, Geneva, Switzerland, https://www.who.int/airpollution/data/cities-2016/en/, 2016.

[44] M.M. Rahman, et al., Recent spatial gradients and time trends in Dhaka, Bangladesh, air pollution and their human health implications, J. Air Waste Manag. Assoc. 69 (2019) 478–501, https://doi.org/10.1080/10962247.2018.1548388. Available:.

[45] M.S. Rahman, et al., How air quality and COVID-19 transmission change under different lockdown scenarios? A case from Dhaka city, Bangladesh, Sci. Total Environ. (2020), https://doi.org/10.1016/j.scitotenv.2020.143161. Available:.

[46] Map of Dinajpur, kantaji.com, Archived from the Original on 13 July, 2011. (Accessed 17 April 2015).

[47] D.E. Alexander, The Third World, Natural Disasters, Kluwer Academic Publishers, 1999, 978-0-412-04751-0.

[48] S.A. Kulp, B.H. Strauss, New elevation data triple estimates of global vulnerability to sea-level rise and coastal flooding, Nat. Commun. 10 (1) (2019) 4844, https://doi.org/10.1038/s41467-019-12808-z.

[49] Report: Flooded Future, Global Vulnerability to Sea Level Rise Worse than Previously Understood, climatecentral.Org, 29 October, 2019. Archived from the original on 2 November (2019). Retrieved 3 November (2019).

[50] J.P. Veefkind, et al., TROPOMI on the ESA Sentinel-5 Precursor: a GMES mission for global observations of the atmospheric composition for climate, air quality and ozone layer applications, Rem. Sens. Environ. 120 (2012) 70–83, https://doi.org/10.1016/j.rse.2012.07.020.

[51] J. Veefkind, et al., TROPOMI on the ESA Sentinel-5 Precursor: a GMES mission for global observations of the atmospheric composition for climate, air quality, and ozone layer applications, Rem. Sens. Environ. 120 (2012) 70–83, https://doi.org/10.1016/j.rse.2012.07.020.

[52] Z.S. Venter, et al., COVID-19 lockdowns cause global air pollution declines, Proc. Natl. Acad. Sci. U. S. A 117 (32) (2020) 18984–18990, https://doi.org/10.1073/pnas.2006853117.

[53] D. Griffin, et al., High-resolution mapping of nitrogen dioxide with TROPOMI: first results and validation over the Canadian oil sands, Geophys. Res. Lett. 46 (2) (2019) 1049–1060, https://doi.org/10.1029/2018GL081095.

[54] A. Lorente, et al., Quantification of nitrogen oxides emissions from build-up of pollution over Paris with TROPOMI, Sci. Rep. 9 (1) (2019) 12, https://doi.org/10.1038/s41598-019-49562-5.

[55] A.I. Prados, et al., Access, visualization, and interoperability of air quality remote sensing data sets via the Giovanni online tool, IEEE J. Sel. Top. Appl. Earth Obs. Rem. Sens. 3 (3) (2010) 359–370, https://doi.org/10.1109/JSTARS.2010.2047940.

[56] J. Acker, R. Soebiyanto, R. Kiang, S. Kempler, Use of the NASA Giovanni data system for geospatial public health research: example of weather-influenza connection, ISPRS Int. J. Geo-Inf. 3 (2014) 1372–1386, https://doi.org/10.3390/ijgi3041372.

[57] J.G. Acker, Using the NASA Giovanni system to assess and evaluate remotely-sensed and model data variables relevant to public health issues, in: F.S. Faruque (Ed.), Geospatial Technology for Human Well-Being and Health, Springer, Cham, 2022, https://doi.org/10.1007/978-3-030-71377-5_8.

[58] L.A. Monteiro, P.C. Sentelhas, G.U. Pedra, Assessment of NASA/POWER satellite-based weather system for Brazilian conditions and its impact on sugarcane yield simulation, Int. J. Climatol. 38 (3) (2018) 1571–1581, https://doi.org/10.1002/joc.5408.

[59] H.H. Hamed, H.J. Jumaah, B. Kalantar, N. Ueda, V. Saeidi, S. Mansor, Z.A. Khalaf, Predicting $PM_{2.5}$ levels over the north of Iraq using regression analysis and geographical information system (GIS) techniques, Geomatics, Nat. Hazards Risk 12 (1) (2021) 1778–1796, https://doi.org/10.1080/19475705.2021.1946602.

[60] A. Tella, A.L. Balogun, I. Faye, Spatio-temporal modelling of the influence of climatic variables and seasonal variation on PM10 in Malaysia using multivariate regression (MVR) and GIS, Geomatics, Nat. Hazards Risk 12 (1) (2021) 443–468, https://doi.org/10.1080/19475705.2021.1879942.

[61] M. Guler, B. Cemek, H. Gunal, Assessment of some spatial climatic layers through GIS and statistical analysis techniques in Samsun Turkey, Meteorol. Appl.: A journal of forecasting, practical applications, training techniques and modelling 14 (2) (2007) 163–169, https://doi.org/10.1002/met.18.

[62] X. Shi, G.P. Brasseur, The response in air quality to the reduction of Chinese economic activities during the COVID-19 outbreak, Geophys. Res. Lett. 47 (2020) e2020GL088070, https://doi.org/10.1029/2020GL088070.

[63] Saiful and Anam, Effect of COVID 19 pandemic induced lockdown (general holiday) on air quality of Dhaka City, Environ. Monit. Assess. 193 (2021) 343, https://doi.org/10.1007/s10661-021-08881-6.

[64] S. Sharma, et al., Effect of restricted emissions during COVID-19 on air quality in India, Sci. Total Environ. 728 (2020) 138878, https://doi.org/10.1016/j.scitotenv.2020.138878.

[65] G. Dantas, et al., The impact of COVID-19 partial lockdown on the air quality of the city of Rio de Janeiro, Brazil, Sci. Total Environ. 729 (2020) 139085, https://doi.org/10.1016/j.scitotenv.2020.139085.

[66] J.M. Baldasano, COVID-19 lockdown effects on air quality by NO_2 in the cities of Barcelona and Madrid (Spain), Sci. Total Environ. 741 (2020) 140353, https://doi.org/10.1016/j.scitotenv.2020.140353.

[67] J. Wang, et al., Impact of COVID-19 on urban air pollution in China, Environ. Res. 195 (2021) 110879, https://doi.org/10.1016/j.envres.2021.110879.

[68] A. Smith, et al., Post-lockdown air quality trends, Atmos. Environ. 265 (2022) 118647, https://doi.org/10.1016/j.atmosenv.2021.118647.

[69] Y. Zhang, et al., Industrial activity and air pollution post-COVID-19 lockdowns, Environ. Pollut. 287 (2022) 117600, https://doi.org/10.1016/j.envpol.2021.117600.

[70] K. Lee, et al., Annual and seasonal NO_2 average in South Asia, Air Quality, Atmosphere & Health 15 (2022) 745–758, https://doi.org/10.1007/s11869-021-01094-4.

[71] S. Gupta, et al., Evaluating air quality post-pandemic in developing countries, Sci. Total Environ. 858 (2023) 159905, https://doi.org/10.1016/j.scitotenv.2022.159905.

[72] M. Masiol, et al., Factors influencing wintertime NO_2 concentrations in urban environments, Atmos. Environ. 171 (2017) 106–117, https://doi.org/10.1016/j.atmosenv.2017.10.047.

[73] S. Squizzato, et al., Seasonal air quality trends and factors, Atmos. Pollut. Res. 9 (2) (2018) 277–287, https://doi.org/10.1016/j.apr.2017.10.008.

[74] W. Huang, et al., The influence of meteorological conditions on pollutant concentrations in asian cities, Environ. Sci. Technol. 55 (7) (2021) 4582–4590, https://doi.org/10.1021/acs.est.0c05658.

[75] M. Khan, et al., Agricultural burning and its impact on air quality in South Asia, J. Environ. Manag. 314 (2023) 115047, https://doi.org/10.1016/j.jenvman.2022.115047.

[76] J.D. Berman, K. Ebisu, Changes in U.S. air pollution during the COVID-19 pandemic, Sci. Total Environ. 739 (2020) 139864, https://doi.org/10.1016/j.scitotenv.2020.139864.

[77] F. Dutheil, J.S. Baker, V. Navel, COVID-19 as a factor influencing air pollution? Environ. Pollut. 263 (2020) 114466 https://doi.org/10.1016/j.envpol.2020.114466.

[78] C. Le Quéré, et al., Temporary reduction in daily global CO_2 emissions during the COVID-19 forced confinement Nature Climate Change 10 (7) (2020) 647–653, https://doi.org/10.1038/s41558-020-0797-x.

[79] R. Bao, A. Zhang, Does lockdown reduce air pollution? Evidence from 44 cities in northern China, Sci. Total Environ. 731 (2020) 139052, https://doi.org/10.1016/j.scitotenv.2020.139052.

[80] B. Silver, G.R. Cass, J.J. Schauer, B. Ostro, Estimates of the mortality impacts of particulate matter air pollution in Los Angeles using a natural experiment, Environ. Sci. Technol. 41 (7) (2007) 2129–2134, https://doi.org/10.1021/es061725z.

[81] J.J. Schwab, Y. Li, M.S. Bae, K.L. Demerjian, Seasonal and diurnal characteristics of particulate matter across New York State, Atmos. Environ. 47 (2012) 3–12, https://doi.org/10.1016/j.atmosenv.2011.11.045.

[82] IEA, Greenhouse Gas Emissions from Energy Highlights, IEA, Paris. Available: https://www.iea.org/data-and-statistics/data-product/greenhouse-gas-emissions-from-energy-highlights.Licence:TermsofUseforNon-CCMaterial.

[83] H. Ritchie, P. Rosado, M. Roser, CO_2 and greenhouse gas emissions, OurWorldInData.org (2023) ourworldindata.org/CO_2-and-greenhouse-gas-emissions [Online Resource].

[84] F.N. Tubiello, C. Rosenzweig, G. Conchedda, K. Karl, J. Gütschow, P. Xueyao, D. Sandalow, Greenhouse gas emissions from food systems: building the evidence base, Environ. Res. Lett. 16 (6) (2021) 065007, https://doi.org/10.1088/1748-9326/ac018e.

[85] USEPA, Landfill Methane Outreach Program, United States Environmental Protection Agency, 2023. Available: https://www.epa.gov/lmop.

[86] R.B. Jackson, M. Saunois, P. Bousquet, J.G. Canadell, B. Poulter, A.R. Stavert, A. Tsuruta, Increasing anthropogenic methane emissions arise equally from agricultural and fossil fuel sources, Environ. Res. Lett. 15 (7) (2020) 071002, https://doi.org/10.1088/1748-9326/ab9ed2.

[87] S. Kirschke, P. Bousquet, P. Ciais, et al., Three decades of global methane sources and sinks, Nat. Geosci. 6 (2013) 813–823. https://doi.org/10.1038/ngeo1955.

[88] A. Tobías, et al., Changes in air quality during the lockdown in Barcelona (Spain) one month into the SARS-CoV-2 epidemic, Sci. Total Environ. 726 (2020) 138540, https://doi.org/10.1016/j.scitotenv.2020.138540.

[89] M. Coccia, Factors determining the diffusion of COVID-19 and suggested strategy to prevent future accelerated viral infectivity similar to COVID, Sci. Total Environ. 729 (2020) 138474, https://doi.org/10.1016/j.scitotenv.2020.138474.

[90] Y. Liu, et al., Impact of relative humidity on $PM_{2.5}$ pollution in China, Atmos. Environ. 125 (2017) 76–83, https://doi.org/10.1016/j.atmosenv.2015.10.017.

[91] Q. Zhang, et al., Influence of low relative humidity on aerosol composition and evolution, Environ. Sci. Technol. 49 (9) (2015) 5466–5474, https://doi.org/10.1021/acs.est.5b00006.

[92] B.J. Finlayson-Pitts, J.N. Pitts Jr., Chemistry of the Upper and Lower Atmosphere: Theory, Experiments, and Applications, Academic Press, 2000, https://doi.org/10.1016/B978-012257060-5/50015-3.

[93] J.H. Seinfeld, S.N. Pandis, Atmospheric Chemistry and Physics: from Air Pollution to Climate Change, John Wiley & Sons, 2016, https://doi.org/10.1002/9781119221166.

[94] M. Jin, R.E. Dickinson, D. Zhang, The footprint of urban areas on global climate as characterized by MODIS, J. Clim. 18 (10) (2005) 1551–1565, https://doi.org/10.1175/JCLI3334.1.

[95] R.A. Pielke, et al., The influence of land-use changes and landscape dynamics on the climate system: relevance to climate-change policy beyond the radiative effect of greenhouse gases, Philos. Trans. R. Soc. London, Ser. A: Math. Phys. Eng. Sci. 360 (1797) (2002) 1705–1719, https://doi.org/10.1098/rsta.2002.1027.

[96] G. He, Y. Pan, T. Tanaka, The short-term impacts of COVID-19 lockdown on urban air pollution in China, Nat. Sustain. 3 (2020) 1005–1011, https://doi.org/10.1038/s41893-020-0581-y.

[97] V. Ramanathan, P.J. Crutzen, J.T. Kiehl, D. Rosenfeld, Aerosols, climate, and the hydrological cycle, Science 294 (5549) (2001) 2119–2124, https://doi.org/10.1126/science.1064034.